

Outage Probability Analysis of NOMA-Enabled Hierarchical UAV Networks with Non-Linear Energy Harvesting

Faïcel Khennoufa¹, Khelil Abdellatif², Metin Ozturk³, Halim Yanikomeroglu⁴, Safwan Alfattani⁵

¹Ecole Nationale Supérieure des Technologies Avancées, Department of Computer Science, Algiers, Algeria.

²LGEERE Laboratory, Department of Electrical Engineering, University of El-Oued, El-Oued, Algeria

³Electrical and Electronics Engineering, Ankara Yıldırım Beyazıt University, Ankara, Türkiye

⁴NTN Lab, Department of Systems and Computer Engineering, Carleton University, Ottawa, Canada

⁵King AbdulAziz University, Saudi Arabia

Abstract

Uncrewed aerial vehicles (UAVs) are expected to enhance connectivity, extend network coverage, and support advanced communication services in sixth-generation (6G) cellular networks, particularly in public and civil domains. Although multi-UAV systems enhance connectivity for IoT networks more than single-UAV systems, energy-efficient communication systems and the integration of energy harvesting (EH) are crucial for their widespread adoption and effectiveness. In this regard, this paper proposes a hierarchical ad hoc UAV network with non-linear EH and non-orthogonal multiple access (NOMA) to enhance both energy and cost efficiency. The proposed system consists of two UAV layers: a cluster head UAV (CHU), which acts as the source, and cluster member UAVs (CMUs), which serve as relays and are capable of harvesting energy from a terrestrial power beacon. For the considered IoT network architecture, the outage probability expressions of ground Internet of things (IoT) devices, each CMU, and the overall outage probability of the proposed system are derived over Nakagami- m fading channels with practical constraints such as hardware impairments and non-linear EH. We compare the proposed system against a non-EH system, and our findings indicate that the proposed system outperforms the benchmark in terms of outage probability.

Index Terms

6G, energy harvesting, outage probability, NOMA, and UAVs.

I. Introduction

UNCREWED aerial vehicles (UAV) communications are pivotal in next-generation wireless networks due to their mobility, low cost, and capacity to cover remote areas [1]. Ad hoc UAV networks provide flexible wireless connectivity with extensive coverage and quick mission adaptability. However, energy scarcity poses a significant challenge, limiting mission duration and effectiveness, necessitating the development of sustainable and cost-effective solutions [2]–[4]. To mitigate this, wireless energy harvesting (EH) leverages ambient radio frequency (RF) signals to provide sustainable energy, enhancing network lifespan and reliability [5]. Additionally, ensuring stable communication is crucial; non-orthogonal multiple access (NOMA) enhances spectral efficiency over orthogonal multiple access (OMA) while requiring careful interference management [2], as it allows multiple users to share the same spectrum simultaneously, improving connectivity. Thus, EH and NOMA enable sustainable, efficient, and resilient UAV communication networks for next-generation wireless communications.

The application of UAVs in wireless networks has attracted a lot of attention recently, inspiring various studies on improving coverage, security, capacity, and reliability [6], [7]. The authors of [8] jointly optimized the placement and power allocation to improve the performance of the NOMA-UAV network. In [9], a UAV-assisted dual-hop radio frequency–underwater wireless optical communication system employing NOMA was investigated, and exact as well as asymptotic expressions for the outage probability were derived under both decode-and-forward (DF) and amplify-and-forward (AF) relaying schemes. The authors of [10] analyzed a UAV-assisted DF NOMA network in terms of outage probability over a Rayleigh fading channel. The authors of [11] optimized the task offloading ratios, user associations, and service caching under constraints related to marine Internet of things (IoT) devices, UAV energy, and cache capacity.

Moreover, multi-UAV systems have gained significant attention due to their ability to coordinate missions and enhance communications efficiency in smart environments. In [12], a multi-hop UAV relay network was proposed to serve ground heterogeneous users lacking direct links, with optimized resource allocation and deployment to meet diverse user needs and reduce outage probability. In [13], a UAV swarm network was analyzed regarding outage probability and capacity by characterizing the effects of UAV-to-UAV interference. Among the various schemes proposed for multi-UAV systems the hierarchical scheme stands out as a prominent approach [14]. In this approach, UAVs are organized into functional layers, which typically include high-altitude leader UAVs and low-altitude follower UAVs.

The leader UAVs handle coordination and communication control, while the follower UAVs perform data collection or relaying tasks [14]. A hierarchical UAV networks provide greater coverage and efficiency by delegating tasks between leader and follower UAVs, thereby reducing power consumption and latency, and enhancing reliability, flexibility, and scalability in large-scale, mission-critical conditions [14].

On the other hand, energy conservation is a major challenge facing UAVs, especially for long-duration missions, due to limited battery capacity and high energy demands of both flight and wireless communications [7]. Therefore, wireless EH has been proposed in the literature as one of the potential solutions to address the energy consumption challenge [15]. In [16], the authors examined the use of RF EH based on ground sources in Internet of things (IoT) systems for UAV-assisted NOMA-based mobile-edge computing. They obtained closed-form expressions for the successful computation and energy consumption probabilities over the Nakagami- m fading channel. The outage probability of UAV-assisted simultaneous wireless information and power transfer (SWIPT) and multiple-input multiple-output (MIMO) with NOMA systems has been studied in different contexts; in [17], a multiple-input single-output (MISO)-NOMA framework for agricultural IoT was analyzed, while in [18], a system with imperfect successive interference cancellation was investigated. A NOMA-assisted full-duplex cooperative UAV-to-UAV communication system was considered in [19], where the UAVs employ an EH framework. The outage expressions for UAV-to-UAV and cellular links were derived through asymptotic analysis [19].

Furthermore, over the last decade, a great amount of effort has been devoted to developing integrated, cost-effective, and energy-efficient RF transceivers. However, these systems suffer from inevitable RF front-end impairments due to component mismatches and manufacturing defects. The authors in [20] explored the impact of hardware impairments (HWI) and imperfect channel state information on the mean square error of over-the-air computation using UAVs. The authors of [21] studied a UAV-enabled IoT network with RF EH and DF relaying under HWI in terms of outage probability, system throughput, and energy efficiency, where the UAV collects energy for IoT devices and forwards their data to the ground base station.

Although previous research introduces the idea of harvesting energy from ground sources, for example, in [7], [15]–[19], they considered linear EH, which is an unrealistic assumption, since numerous experiments on real electromagnetic circuits have demonstrated the non-linearity of their input and output characteristics. In addition, most existing works on UAV-assisted communications consider either a single-UAV system or a flat multi-UAV system, while assuming ideal HWI and either ignoring EH or adopting linear EH systems [6]–[14]. Although wireless EH techniques with or without NOMA have been analyzed for a UAV-assisted system individually [7], [15]–[19], a hierarchical system of multiple UAVs using NOMA and non-linear EH and HWI is not explored in the existing literature, to the best of the authors' knowledge. In practical RF EH techniques, non-linear EH is a major factor, and HWIs in transceivers are inevitable components in wireless communication systems. However, analysis of non-linear EH and HWIs is rarely explored in the analysis of multi-UAV-assisted wireless communication networks. Motivated by these limitations, this work investigates a hierarchical UAV-assisted wireless communication system incorporating NOMA, non-linear EH, and HWIs, providing a more practical framework for the analysis of multi-UAV-assisted wireless communication networks. The system comprises two levels of UAVs: a cluster head UAV (CHU) acting as the source, and cluster member UAVs (CMUs) that harvest energy from the power beacon (PB) transmitted energy and utilize this harvested energy to relay information to ground IoT devices. We employ the NOMA technique to enhance spectrum efficiency while considering the effects of HWI on the proposed system with EH in a practical scenario. The main contributions of this paper are given as follows:

- We propose a joint design that integrates non-linear EH from PB signals with NOMA, offering enhanced spectrum efficiency and sustainable energy management in hierarchical ad hoc UAV networks. To ensure a more realistic and practical evaluation, we also consider the impact of HWI on the system.
- We derive the outage probability of the proposed hierarchical ad hoc UAV network that incorporates non-linear EH and NOMA in the presence of HWI. Furthermore, we obtain the outage probability of the system for a single CMU (called CMU outage probability), as well as the overall outage probability of a hierarchical ad hoc UAV network (i.e., network outage probability).
- To demonstrate the superiority of the proposed system, we compare it against two benchmark schemes: an ad hoc hierarchical UAV network using non-linear EH with NOMA, and a ground-based EH system where UAVs harvest energy directly from terrestrial transmitters.

The rest of the paper is organized as follows: The proposed hierarchical ad hoc UAV network with non-linear EH and NOMA under the impact of HWI is presented in Section II. We derive the outage probability of the proposed system in Section III. Finally, Section IV presents and discusses the simulation results, while Section V offers the conclusion.

II. System Model

As illustrated in Fig. 1, we consider a hierarchical ad hoc UAV network designed to serve a set of ground IoT devices. The network consists of a CHU, L CMUs, indexed by $l = 1, 2, \dots, L$, M ground IoT devices, indexed by

$n = 1, 2, \dots, M$, and a PB. The CHU is assumed to serve as the communication source and resource management coordinator for the cluster members, while the cluster members (i.e., CMUs) act as relay UAVs to forward data to the ground IoT devices. In this scenario, we consider the following assumptions: 1) The CHU is a hovering platform at a fixed location, moving slowly enough to be considered stationary while providing coverage. 2) All nodes are equipped with one (transmit/receive) antenna. 3) Perfect CSI is available at all nodes, and the communication links experience Nakagami- m fading. 4) The CMUs operate in the DF protocol and HD mode. 5) HWI is considered at all nodes. We assume that CMUs are equipped with batteries to harvest and store wireless energy, while the CHU is equipped with solar cells, enabling it to harvest energy and operate sustainably. It is assumed that the CMUs harvest energy transmitted by the PB using the TS protocol and store it in their batteries, which is then used to power subsequent transmissions to ground IoT devices.

Considering the channel scenarios in [14], the link between the CHU and CMUs, and CMUs in the UAV ad hoc network may establish a direct air-to-air (A2A) connection, which can be considered a line-of-sight (LoS) link altogether. In contrast, the link between the CMUs and ground IoT devices, PB and ground CMUs may establish an air-to-ground (A2G) connection, which can be considered a mixed LoS and non-LoS (NLoS). Thus, the path-loss coefficient of the A2A and A2G links can be formulated, respectively, as [14], [22]

$$\Upsilon_l = \zeta_0 d_l^{-\beta} \quad (1)$$

and

$$\Upsilon_{\varpi} = (\zeta_1 \Lambda_{\text{LoS}} + \zeta_2 \Lambda_{\text{NLoS}}) d_{\varpi}^{-\beta}, \varpi = \{n, e\}, \quad (2)$$

where ζ_0 , ζ_1 , and ζ_2 are the additional path-loss of the channel under LoS and NLoS transmission conditions, β is the path-loss exponent of the channel. d_l is the Euclidean distance between the CHU and CMUs. d_{ϖ} is the Euclidean distance between the CMUs and ground IoT devices, and the PB and CMUs. Λ_{LoS} and Λ_{NLoS} are the LoS and NLoS probabilities. Therefore, the probability of LoS channel occurrence can be written as

$$\Lambda_{\text{LoS}} = \frac{1}{1 + \xi_1 \exp\left(-\xi_2 \left[\arcsin\left(\frac{H}{d_n}\right) - \xi_1\right]\right)}, \quad (3)$$

where H is the altitude of the CMUs, ξ_1 and ξ_2 are constant values depending on the environment [14]. Accordingly, the probability of NLoS can be given as

$$\Lambda_{\text{NLoS}} = 1 - \Lambda_{\text{LoS}}. \quad (4)$$

In the present investigation, we consider a downlink NOMA with a time switching (TS) protocol, in which the CHU serves ground IoT devices through CMUs. Let T be the total transmission time. In the first ρT time slots, the CMUs harvest energy from PB. In the first $(1-\rho)T/2$ of the remaining time, the CHU sends superimposed coding (SC) information to the CMUs based on NOMA. The signals are decoded using successive interference cancellation (SIC). Then, in the last $(1-\rho)T/2$ time slot, the CMUs use the harvested energy to deliver this information signal to the ground IoT devices. In the TS protocol, information decoding and EH are performed in distinct time slots. In the first ρT time slot, the CMUs collect energy from PB. The received signal at the CMUs for EH and information decoding can be written by

$$y_l = (\sqrt{P_t} X_S + v_{t,l}) g_l + v_{r,l} + \mu_l, \varsigma = \{\rho, \iota\}, \quad (5)$$

where $X_S = \sum_{n=1}^M \sqrt{\alpha_n} x_n$. α_n are the power allocation coefficients for the signal of ground IoT devices. Besides, we have $\sum_{n=1}^M \alpha_n = 1$. g_l follows instantaneous Nakagami- m fading with Ω_l spread and m_l shape parameters, where $\Omega_l = \Upsilon_l$ and m_l are assumed to be greater than 1, as in [23]. P_t is the CHU total transmit power, ρ is the TS factor ($0 \leq \rho \leq 1$), and μ_l is the additive white Gaussian noise (AWGN), which follows $\mu_l \sim \mathcal{CN}(0, \sigma_l^2)$. $v_{t,l}$ and $v_{r,l}$ are distortion noises at the transmitter and receiver, respectively, which occur due to the HWI at transceivers, such as oscillator phase noise, high power amplifier distortion, and in-phase and quadrature-phase imbalance. The distortion noises are defined as $v_{t,l} \sim \mathcal{CN}(0, \iota P_t k_{t,l}^2)$ and $v_{r,l} \sim \mathcal{CN}(0, \iota P_t k_{r,l}^2 |g_l|^2)$, where $k_{t,l}^2$ and $k_{r,l}^2$ represent levels of impairment at the transmitter and receiver, respectively [24], [25]. It is demonstrated in [24]–[26] that the impact of the transceiver HWI can be characterized by the aggregate level of impairments and can be written as $k_l^2 = k_{t,l}^2 + k_{r,l}^2$.

Considering the non-linear feature of a practical EH circuit, the EH expressions during the EH phase (i.e., first ρT time slot) at the CMUs can be given as in [25] by

$$E_{\text{EH}} = \begin{cases} \eta \rho P_t |g_e|^2 T, & P_t |g_e|^2 \leq P_{\text{th}}, \\ \eta \rho P_{\text{th}} T, & P_t |g_e|^2 > P_{\text{th}}, \end{cases} \quad (6)$$

where $0 \leq \eta \leq 1$ is the energy conversion efficiency factor and P_{th} is the saturation threshold. g_e is the channel between PB and CMUs, which follows instantaneous Nakagami- m fading with Ω_e spread and m_e shape parameters, where $\Omega_e = \Upsilon_e$ and m_e are assumed to be greater than 1, as in [23].

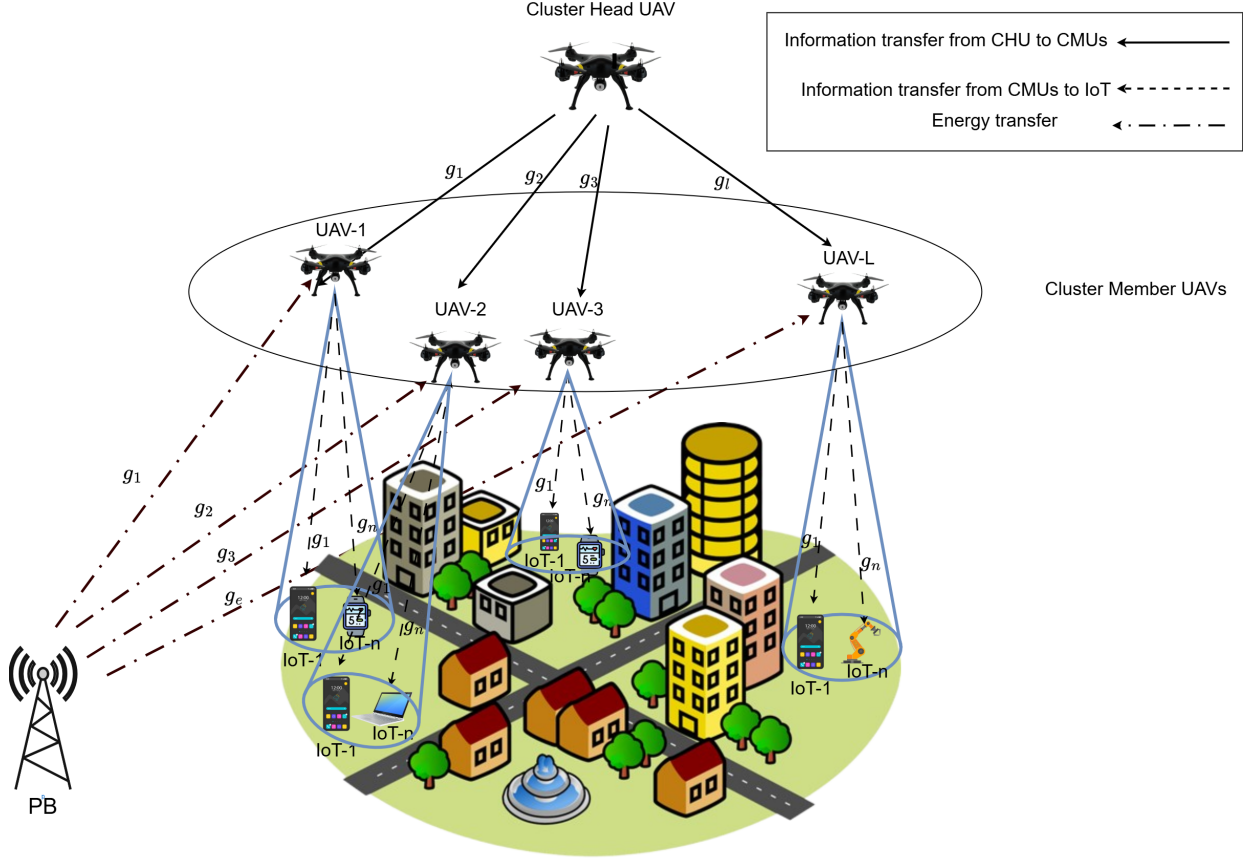


Fig. 1: Hierarchical ad hoc UAV network with EH system model.

The transmission power of the CMUs through the harvested energy is given by

$$P_{EH} = \frac{E_{EH}}{T(1-\rho)/2} = \begin{cases} \frac{2\eta\rho P_t |g_e|^2}{1-\rho}, & P_t |g_e|^2 \leq P_{th}, \\ \frac{2\eta\rho P_{th}}{1-\rho}, & P_t |g_e|^2 > P_{th}. \end{cases} \quad (7)$$

At CMUs, the signal is decoded by using SIC. Hence, the signal-to-interference-plus-noise ratio (SINR) of the signal x_n is given by

$$\gamma_{l,n} = \frac{\iota P_t |g_l|^2 \alpha_n}{\iota P_t |g_l|^2 \sum_{n+1}^M \alpha_n + \iota k_l^2 P_t |g_l|^2 + \sigma_l^2}. \quad (8)$$

In the remaining time (i.e., first $(1-\rho)T/2$ of the remaining time), the CMUs re-encode the detected signals similar to the first time slot and forward it to the ground IoT devices using the EH power. The received signal at n th ground IoT devices can be written by

$$y_n = (\sqrt{P_{EH}} X_S + v_{t,n}) g_n + v_{r,n} + \mu_n, \quad (9)$$

where g_n follows Nakagami- m fading with spread $\Omega_n = \Upsilon_n$ and m_n shape parameters, which is assumed to be greater than 1, as in [23]. $\mu_n \sim \mathcal{CN}(0, \sigma_n^2)$ is the AWGN. $v_{t,n} \sim \mathcal{CN}(0, P_{EH} k_{t,n}^2)$ and $v_{r,n} \sim \mathcal{CN}(0, P_{EH} k_{r,n}^2 |g_n|^2)$ are distortion noises at the transceiver, respectively, where $k_{t,n}^2$ and $k_{r,n}^2$ denote the transceiver impairment levels, respectively. The aggregate HWI is $k_n^2 = k_{t,n}^2 + k_{r,n}^2$ [24]–[26].

Similar to the first time slot, the signals are detected using SIC, respectively, at the n th ground IoT device. Accordingly, their SINRs are given by

$$\gamma_n = \begin{cases} \gamma_n^A, & P_t |g_l|^2 \leq P_{th}, \\ \gamma_n^B, & P_t |g_l|^2 > P_{th}, \end{cases} \quad (10)$$

where $\gamma_n^A = \frac{\eta\rho P_t |g_n|^2 |g_l|^2 \alpha_n}{\eta\rho P_t |g_n|^2 |g_l|^2 \sum_{i=n+1}^M \alpha_i + k_n^2 \eta\rho P_t |g_n|^2 |h_l|^2 + \sigma_n^2}$ and $\gamma_n^B = \frac{\eta\rho P_{th} |g_n|^2 \alpha_n}{\eta\rho P_{th} |g_n|^2 \sum_{i=n+1}^M \alpha_i + k_n^2 \eta\rho P_{th} |g_n|^2 + \sigma_n^2}$.

III. Outage Probability analysis

This section derives the outage probability of the hierarchical ad hoc UAV network with non-linear EH by calculating the analytical expressions for each ground IoT device within one CMU. We take into account the effect of non-ideal

conditions (i.e., HWI) in our derivations. Then, we obtain the outage probability of the system at a single CMU and the overall outage probability of a hierarchical ad hoc UAV network (i.e., outage probability at L CMUs).

The probability density function (PDF) and cumulative distribution function (CDF) of h can be, respectively, given as

$$f_{|h|^2}(x) = \left(\frac{m}{\Omega}\right)^m \frac{x^{m-1}}{\Gamma(m)} e^{-\frac{m}{\Omega}x} \quad (11)$$

and

$$F_{|h|^2}(x) = \frac{\Upsilon(m, \frac{m}{\Omega}x)}{\Gamma(m)}, \quad (12)$$

where $\Gamma(m) = \int_0^\infty x^{m-1}e^{-x}dx$ and $\Upsilon(m, x) = \int_0^x x^{m-1}e^{-x}dx$ represent the Gamma function and lower incomplete Gamma function, respectively.

A. Outage Probability of NOMA Devices

In the first and second time slots, an outage does not occur if the CMUs and ground IoT devices are able to successfully decode all messages x_n . In particular, the end-to-end (E2E) outage probability of the n th ground IoT device is expressed by

$$P_n(\text{out}) = 1 - (1 - P_{l,n}^I(\text{out})) (1 - P_n^{II}(\text{out})), \quad (13)$$

where $P_{l,n}^I(\text{out})$ and $P_n^{II}(\text{out})$ denote the outage probabilities at the CMU and ground IoT device corresponding to the first and second $(1-\rho)T/2$ slots, respectively. The outage probability at the CMU is given by

$$P_{l,n}^I(\text{out}) = \frac{\Upsilon(m_l, \frac{m_l}{\Omega_l} \hat{\gamma}_{l,n})}{\Gamma(m_l)}, \quad (14)$$

where $\hat{\gamma}_{l,n} = \max\{\mathcal{U}_{l,n}\}$, $\mathcal{U}_{l,n} = \frac{\sigma_l^2 \varphi_{l,n}}{(\alpha_n - \sum_{i=n+1}^M \alpha_i \varphi_{l,n} + k_l^2 \varphi_{l,n}) \iota P_t}$. and $\varphi_{l,n} = 2^{2r_p} - 1$, where r_p denote the target rates of x_n .

Theorem 1: The outage probability at the n^{th} ground IoT device occurs when the messages are not successfully decoded. Hence, the outage probability at the second $(1-\rho)T/2$ time slot can be expressed as

$$P_n^{II}(\text{out}) = 1 - \prod_n^M (1 - \aleph_1 - \aleph_2(1 - \aleph_3)), \quad (15)$$

where $\aleph_1 = \int_0^{\frac{P_{\text{th}}}{P_t}} \frac{\Upsilon\left(m_l, \frac{m_l \mathcal{U}_n^A}{\Omega_l x}\right)}{\Gamma(m_l)} \cdot \frac{m_n^{m_n} x^{m_n-1}}{\Gamma(m_n) \Omega_n^{m_n}} e^{-\frac{m_n}{\Omega_n} x} dx$, $\aleph_2 = \frac{\Upsilon(m_n, \frac{m_n \mathcal{U}_n^B}{\Omega_n})}{\Gamma(m_n)}$, $\aleph_3 = \frac{\Upsilon(m_l, \frac{m_l \chi}{\Omega_l})}{\Gamma(m_l)}$, $\mathcal{U}_n^A = \frac{\sigma_n^2 \varphi_n}{(\alpha_n - \varphi_n \sum_{i=n+1}^M \alpha_i + k_n^2 \varphi_n) \eta \rho P_t}$, $\mathcal{U}_n^B = \frac{\sigma_n^2 \varphi_n}{(\alpha_n - \varphi_n \sum_{i=n+1}^M \alpha_i + k_n^2 \varphi_n) \eta \rho P_{\text{th}}}$, and $\chi = \frac{P_{\text{th}}}{P_t}$.

Hence, to find the E2E outage probability of the n th ground IoT device, we substitute (14) and (15) into (13).

B. CMU Outage Probability

A single CMU is considered in outage if the transmission to at least one associated ground IoT device fails, i.e., if the device cannot correctly decode its intended signal. Thus, the CMU outage probability is expressed by

$$P_{\text{CMU},l}(\text{out}) = 1 - \prod_n^M (1 - P_n(\text{out})), \quad (16)$$

where $P_n(\text{out})$ is the outage probability of the n th ground IoT device, which is given in (15).

C. Overall Outage Probability

The overall outage probability denotes the probability that at least one CMU system fails to serve its ground IoT devices. Hence, the overall outage probability of L CMUs can be formulated by

$$P_{\text{sys}}(\text{out}) = 1 - \prod_l^L (1 - P_{\text{CMU},l}(\text{out})). \quad (17)$$

IV. Numerical Results

In this section, we evaluate the proposed hierarchical ad hoc UAV network with non-linear EH and NOMA under the effect of HWI. All parameters used in the simulations are given in Table I.

Fig. 2 presents the outage probability performance of two ground IoT devices that are derived from the expression in (16) with different $P_{\text{th}} = \{2, 5, 20\}$ dBm, when HWI factor $K = \{0, 0.15\}$ as in [24]. The numerical results closely match the simulation results, validating our analytical expressions. As the transmit power increases, the outage probability consistently decreases for all threshold settings, confirming that higher power improves link reliability. However, larger threshold values result in higher outage probabilities since more stringent decoding requirements are imposed on the receivers. At high transmit power levels, the curves approach an outage floor, indicating that system performance

TABLE I: Simulation Parameters.

Parameter	Value	Parameter	Value
q_{CHU}	(40, 20, 50)	L	5
$q_{\text{CMU},l}$	(15, 25, 30)	H	20
q_1	(65, 74, 0)	M	2
q_2	(55, 70, 0)	P_{th}	5 dBm
ξ_1	9.6	$\zeta_0 = \zeta_1$	1
ξ_2	0.28	ζ_2	0.2
ρ	0.1	η	0.95
$K = k_l = k_n$	0.15	$m = m_l = m_n$	1.5

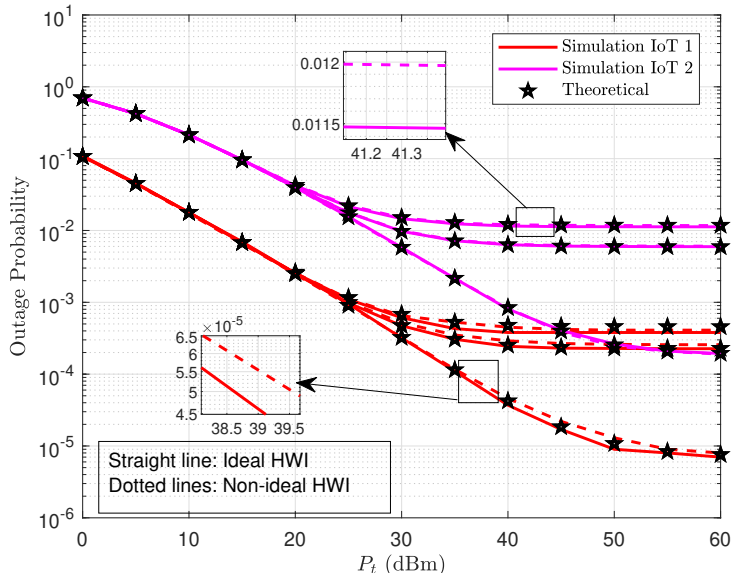


Fig. 2: Outage probability performance of two ground IoT devices with different thresholds and HWI.

becomes limited by threshold P_{th} and inherent system constraints rather than transmit power. This behavior reflects the saturation effect of realistic rectifier circuits used in EH modules. Furthermore, we observe that performance deteriorates in the non-ideal case of HWI.

Fig. 3 presents the CMU outage probability performance of for different Nakagami- m shape parameters, $P_{\text{th}} = \{2, 5, 20\}$ dBm, with $K = 0.15$. It is observed that the CMU outage probability decreases with increasing transmit power for both NOMA systems; i.e., with and without EH. The system with EH consistently outperforms the system without EH across different threshold levels P_{th} , with an estimated gain of 10 dB, highlighting the performance benefits of incorporating EH. It is worth noting that at high transmit power levels, the EH system reflects the saturation effect of realistic rectifier circuits used in EH, which causes an outage floor.

The CMU outage probability performance of for different Nakagami- m shape parameters, $m = \{1, 1.5, 2\}$, with $K = 0.15$ is illustrated in Fig. 4. The analysis considers both integer and non-integer values of m , demonstrating the generality of the derived expressions. We observe that the shape parameter m plays a key role in determining the diversity order of the system. As m increases, the CMU outage probability curves become steeper, indicating an improvement in diversity gain. This behavior can be attributed to the fact that larger values of m correspond to less severe fading conditions in the Nakagami- m channel model. Consequently, the occurrence of deep fades is reduced and the average received signal power is increased, resulting in a lower outage probability and enhanced link reliability. Moreover, we find that the NOMA system with EH outperforms the system without EH for different values of m , with an estimated gain of 8-12 dB, highlighting the performance benefits of EH.

Furthermore, to illustrate the trade-off between system performance and the number of CMUs used to enhance coverage, Fig. 5 shows the overall outage probability for different numbers of CMUs, $L = \{4, 6, 8\}$. It can be shown that increasing the number of CMUs reduces overall outage performance because, as more CMUs participate in the relaying process, the system becomes more prone to link failures, increasing the possibility that at least one CMU will experience unfavorable channel conditions or an outage. This occurs because adding more CMUs increases the possibility that one of them may encounter a unfavorable link, which boosts the overall outage probability. Therefore, it is important to avoid excessively increasing the number of CMUs.

Fig. 6 shows the overall outage probability versus the HWI level K with different $P_{\text{th}} = \{5, 30\}$ dBm. The findings

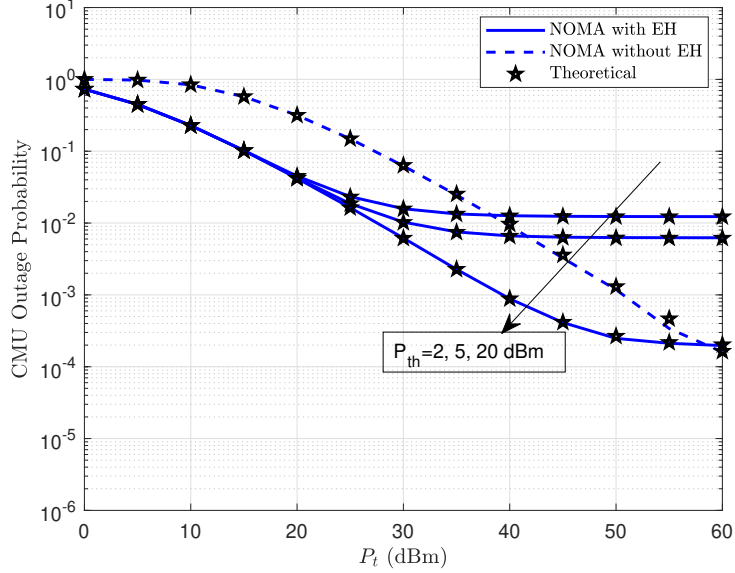


Fig. 3: CMU Outage probability performance with different $P_{th} = \{2, 5, 20\}$ dBm values, when $K = 0.15$: Comparison between NOMA with EH and without EH.

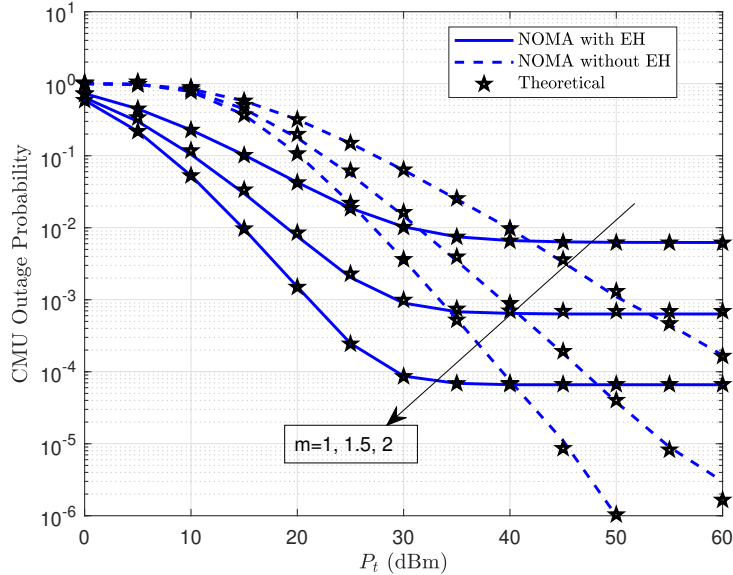


Fig. 4: CMU Outage probability performance with different $m = \{1, 1.5, 2\}$ values, when $K = 0.15$: Comparison between NOMA with EH and without EH.

demonstrate the effect of HWI on system reliability in terms of overall outage performance. As K grows, the overall outage probability gradually degrades, indicating that HWI causes non-negligible performance loss even at modest impairment levels. This emphasises the need of incorporating HWIs into the design and analysis of real wireless communication systems. It is also worth noting that increasing the saturation threshold (P_{th}) improves outage performance and mitigates the impact of HWI. This is because a higher saturation threshold allows more harvested energy to be effectively utilized, enhancing transmission power and improving signal robustness against distortion and noise.

V. Conclusion

This study proposed a hierarchical ad hoc UAV network with non-linear EH and NOMA to enhance both energy and cost efficiency. In the proposed system, we used a two-layer UAV system: the CHU acts as a source, and the

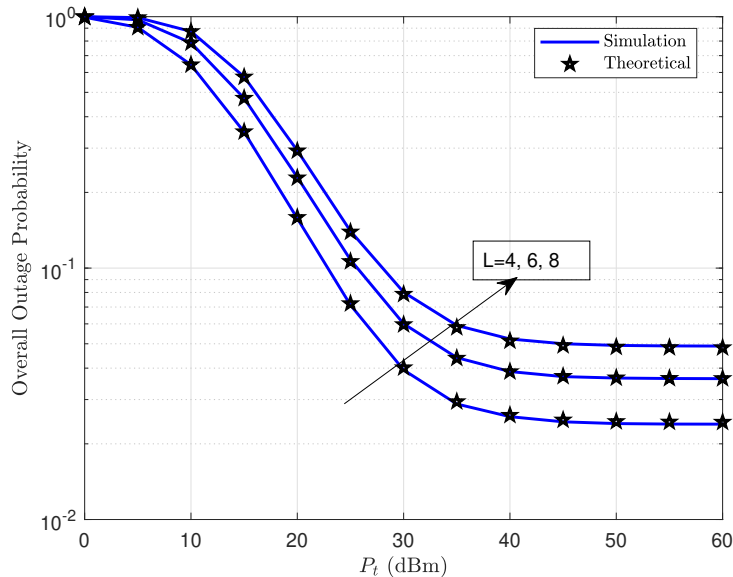


Fig. 5: Overall outage probability for RSMA and NOMA with different numbers of CMU, $L = \{4, 6, 8\}$.

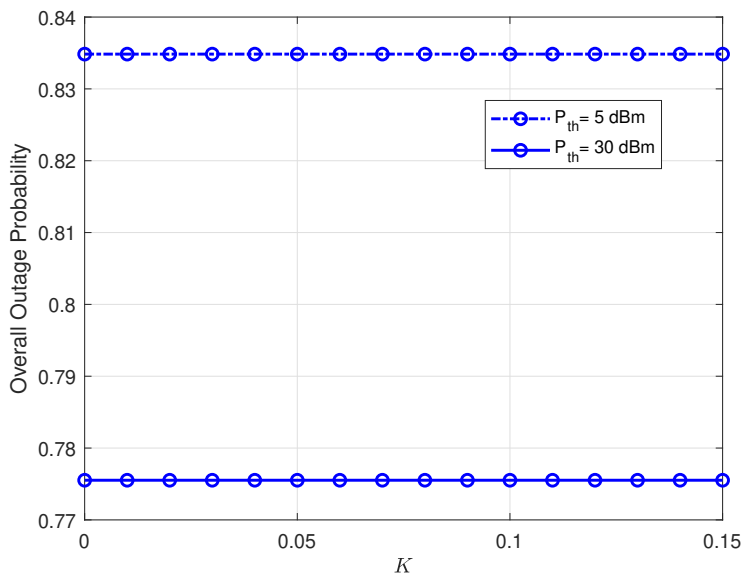


Fig. 6: Overall outage probability w.r.t. HWI (K) with different $P_{th} = \{5, 30\}$ dBm.

CMUs act as relays that can harvest power from the ground transmission. Considering practical conditions such as non-linear EH and hardware impairments, we derived the outage probabilities corresponding to the ground IoT devices, each CMU, and the overall system performance under Nakagami- m fading channels. The proposed system is compared with a non-EH system. The findings revealed that the NOMA outperforms the systems without EH, with an estimated gain between 8 and 12 dB. Increasing the number of CMUs improves coverage but also raises the overall outage probability, thereby excessively increasing the number of CMUs should be avoided. Increasing the HWI level degrades system reliability, highlighting the need to account for hardware impairments.

References

- [1] M. Ozturk, M. Salamatmoghadasi, and H. Yanikomeroglu, "Integrating terrestrial and non-terrestrial networks for sustainable 6G operations: a latency-aware multi-tier cell-switching approach," *IEEE Network* (Early Access), 2025.
- [2] F. Khennoufa, K. Abdellatif, H. Yanikomeroglu, M. Ozturk, T. Elganimi, F. Kara, and K. Rabie, "A multi-layer non-terrestrial networks architecture for 6G and beyond under realistic conditions and with practical limitations," *IEEE Internet of Things Mag.*, vol. 8, no. 5, pp. 136–143, 2025.
- [3] —, "Multi-layer network formation through HAPS base station and transmissive RIS-equipped UAV," in *IEEE Wirel. Commun.*

- Net. Conf. (WCNC), 2025, pp. 1–6.
- [4] B. Karaman, I. Basturk, S. Taskin, E. Zeydan, F. Kara, E. A. Beyazit, M. Camelo, E. Björnson, and H. Yanikomeroglu, “Solutions for sustainable and resilient communication infrastructure in disaster relief and management scenarios,” *IEEE Commun. Surv. Tutor.*, vol. 28, pp. 716–760, 2026.
 - [5] Q. M. Khalaf, A. Sali, A. Ismail, M. Y. Ahmad, Y. S. Hussein, and J. A. Shah, “Advanced nonlinear optimization techniques in SWIPT: a review,” *IEEE Access*, vol. 12, pp. 192 743–192 766, 2024.
 - [6] J. Xu, K. Ota, and M. Dong, “Ideas in the air: unmanned aerial semantic communication for post-disaster scenarios,” *IEEE Wirel. Commun. Lett.*, vol. 14, no. 6, pp. 1598–1602, 2025.
 - [7] M. Ahmed, A. A. Soofi, F. Khan, S. Raza, W. U. Khan, L. Su, F. Xu, and Z. Han, “Toward a sustainable low-altitude economy: a survey of energy-efficient RIS-UAV networks,” *IEEE Internet of Things J.*, vol. 12, no. 24, pp. 51 951–51 975, 2025.
 - [8] X. Liu, J. Wang, N. Zhao, Y. Chen, S. Zhang, Z. Ding, and F. R. Yu, “Placement and power allocation for NOMA-UAV networks,” *IEEE Wirel. Commun. Lett.*, vol. 8, no. 3, pp. 965–968, 2019.
 - [9] X. Pi, S. Jia, D. Zhang, P. Du, Y. Xu, Y. Lou, and X. Li, “Outage probability of UAV-assisted dual-hop RF-UWOC systems leveraging NOMA,” *IEEE Trans. Veh. Tech.*, vol. 75, no. 2, pp. 3318–3323, 2026.
 - [10] D. Bepari, S. Mondal, B. Acharya, and D. Dubey, “UAV-Assisted NOMA-Enabled Relay Communication,” *Int. J. Commun. Syst.*, vol. 39, no. 1, p. e70322, 2026.
 - [11] Y. Zhang, Z. Na, S. Li, B. Lin, Y. Lin, and A. Nallanathan, “Joint service caching and task offloading for multi-UAV-assisted offshore edge computing networks,” *IEEE Trans. Veh. Tech.*, vol. 74, no. 12, pp. 19 667–19 680, 2025.
 - [12] W. Pan, N. Lv, B. Hou, and Z. Ren, “Resource allocation and outage probability optimization method for multi-hop UAV relay network for servicing heterogeneous users,” *IEEE Trans. Net. Sci. Eng.*, vol. 11, no. 3, pp. 2769–2781, 2024.
 - [13] W. J. Lau, J. M.-Y. Lim, C. Y. Chong, N. S. Ho, and T. W. M. Ooi, “General outage probability model for UAV-to-UAV links in multi-UAV networks,” *Comput. Net.*, p. 109752, 2023.
 - [14] X. Yang, B. Han, G. Zhang, P. Zheng, J. Bai, and D. Qin, “NOMA-assisted routing algorithm design for UAV ad hoc relay networks,” *IEEE Sens. J.*, vol. 23, no. 3, pp. 3296–3312, 2023.
 - [15] T. Ojha, T. P. Raptis, A. Passarella, and M. Conti, “Wireless power transfer with unmanned aerial vehicles: state of the art and open challenges,” *Pervasive Mob. Comput.*, vol. 93, p. 101820, 2023.
 - [16] A.-N. Nguyen, D.-B. Ha, V. N. Vo, V.-T. Truong, D.-T. Do, and C. So-In, “Performance analysis and optimization for IoT mobile edge computing networks with RF energy harvesting and UAV relaying,” *IEEE Access*, vol. 10, pp. 21 526–21 540, 2022.
 - [17] Y. He, F. Huang, D. Wang, and R. Zhang, “Outage probability analysis of MISO-NOMA downlink communications in UAV-assisted Agri-IoT with SWIPT and TAS enhancement,” *IEEE Trans. Net. Sci. Eng.*, vol. 12, no. 3, pp. 2151–2164, 2025.
 - [18] H. Çağiran, O. Kucur, and S. Büyükçorak, “Outage performance of UAV-assisted relaying MIMO-NOMA networks with SWIPT in Rician fading channels,” *AEÜ Int. J. Electron. Commun.*, vol. 193, p. 155713, 2025.
 - [19] R. Bajpai, A. S. Shaikh, and N. Gupta, “Wireless powered NOMA assisted full-duplex cooperative U2U communications system with fluctuating two-ray channel,” *IEEE Access*, vol. 13, pp. 54 069–54 079, 2025.
 - [20] H. Alsmadi, E. Saleh, M. Alsmadi, and S. Ikki, “Hardware impairments effects on over the air system assisted by unmanned aerial vehicle,” *IEEE Commun. Lett.*, vol. 28, no. 7, pp. 1609–1613, 2024.
 - [21] G. K. Pandey, D. S. Gurjar, S. Yadav, and S. Solanki, “UAV-empowered IoT network With hardware impairments and shadowing,” *IEEE Sens. Lett.*, vol. 7, no. 7, pp. 1–4, 2023.
 - [22] B. Ning, M. Yi, Y. Xu, J. Li, and W. Hao, “UAV-assisted AmBC network: performance analysis in nakagami- m fading channel,” *IEEE Trans. Veh. Tech.*, vol. 74, no. 5, pp. 6966–6978, 2025.
 - [23] M. Babaei, Ü. Aygözü, and E. Basar, “BER analysis of dual-hop relaying with energy harvesting in nakagami- m fading channel,” *IEEE Trans. Wirel. Commun.*, vol. 17, no. 7, pp. 4352–4361, 2018.
 - [24] S. Beddiaf, A. Khelil, F. Khennoufa, F. Kara, H. Kaya, X. Li, K. Rabie, and H. Yanikomeroglu, “A unified performance analysis of cooperative NOMA with practical constraints: hardware impairment, imperfect SIC and CSI,” *IEEE Access*, vol. 10, pp. 132 931–132 948, 2022.
 - [25] F. Khennoufa, A. Khelil, S. Beddiaf, F. Kara, K. Rabie, H. Kaya, A. Emir, S. Ikki, and H. Yanikomeroglu, “Wireless powered cooperative communication network for dual-hop uplink NOMA with IQI and SIC imperfections,” *IEEE Access*, vol. 11, pp. 76 506–76 523, 2023.
 - [26] C. Studer, M. Wenk, and A. Burg, “MIMO transmission with residual transmit-RF impairments,” in *IEEE ITG WSA*, 2010, pp. 189–196.